



**HAL**  
open science

## **Rainfall control on Amazon sediment flux: synthesis from 20 years of monitoring**

Elisa Armijos, Alain Crave, Jhan Carlo Espinoza, Naziano Filizola, Raul Espinoza-Villar, Irma Ayes, Paula Fonseca, Pascal Fraizy, Omar Gutierrez, Philippe Vauchel, et al.

### ► **To cite this version:**

Elisa Armijos, Alain Crave, Jhan Carlo Espinoza, Naziano Filizola, Raul Espinoza-Villar, et al.. Rainfall control on Amazon sediment flux: synthesis from 20 years of monitoring. *Environmental Research Communications*, 2020, 2 (5), pp.051008. <10.1088/2515-7620/ab9003>. <insu-02569689>

**HAL Id: insu-02569689**

**<https://insu.hal.science/insu-02569689v1>**

Submitted on 11 May 2020

**HAL** is a multi-disciplinary open access archive for the deposit and dissemination of scientific research documents, whether they are published or not. The documents may come from teaching and research institutions in France or abroad, or from public or private research centers.

L'archive ouverte pluridisciplinaire **HAL**, est destinée au dépôt et à la diffusion de documents scientifiques de niveau recherche, publiés ou non, émanant des établissements d'enseignement et de recherche français ou étrangers, des laboratoires publics ou privés.



Distributed under a Creative Commons CC BY 4.0 - Attribution - International License

ACCEPTED MANUSCRIPT • OPEN ACCESS

## Rainfall control on Amazon sediment flux: synthesis from 20 years of monitoring

To cite this article before publication: Elisa Armijos *et al* 2020 *Environ. Res. Commun.* in press <https://doi.org/10.1088/2515-7620/ab9003>

### Manuscript version: Accepted Manuscript

Accepted Manuscript is “the version of the article accepted for publication including all changes made as a result of the peer review process, and which may also include the addition to the article by IOP Publishing of a header, an article ID, a cover sheet and/or an ‘Accepted Manuscript’ watermark, but excluding any other editing, typesetting or other changes made by IOP Publishing and/or its licensors”

This Accepted Manuscript is © 2020 The Author(s). Published by IOP Publishing Ltd.

As the Version of Record of this article is going to be / has been published on a gold open access basis under a CC BY 3.0 licence, this Accepted Manuscript is available for reuse under a CC BY 3.0 licence immediately.

Everyone is permitted to use all or part of the original content in this article, provided that they adhere to all the terms of the licence <https://creativecommons.org/licenses/by/3.0>

Although reasonable endeavours have been taken to obtain all necessary permissions from third parties to include their copyrighted content within this article, their full citation and copyright line may not be present in this Accepted Manuscript version. Before using any content from this article, please refer to the Version of Record on IOPscience once published for full citation and copyright details, as permissions may be required. All third party content is fully copyright protected and is not published on a gold open access basis under a CC BY licence, unless that is specifically stated in the figure caption in the Version of Record.

View the [article online](#) for updates and enhancements.

## Rainfall control on Amazon sediment flux: synthesis from 20 years of monitoring

Armijos E<sup>1,2</sup>, Crave A<sup>3</sup>, Espinoza J C<sup>4</sup>, Filizola, N<sup>2</sup>, Espinoza-Villar R<sup>5</sup>, Ayes I<sup>6</sup>, Fonseca P<sup>6</sup>, Fraizy P<sup>7</sup>, Gutierrez O<sup>8</sup>, Vauchel P<sup>7</sup>, Camenen B<sup>9</sup>, Martinez J M<sup>7</sup>, Dos Santos A<sup>6,10</sup>, Santini W<sup>7</sup>, Cochonneau G<sup>7</sup>, Guyot J L<sup>7</sup>.

1. Instituto Geofísico del Perú (IGP), Lima, Peru.
2. Universidade Federal do Amazonas (UFAM), Manaus, Brazil.
3. Univ. Rennes, CNRS, Géoscience Rennes, UMR 6118, 3500 Rennes, France.
4. Univ. Grenoble Alpes, IRD, CNRS, Grenoble INP, Institute des Géosciences de l'Environnement (IGE, UMR 5001), 38000 Grenoble, France.
5. Univ. Nacional Agraria La Molina. UNALM . Av. La Molina s/n. Lima-Per
6. CLIAMB. Instituto Nacional de Pesquisas da Amazônia (INPA), Universidade do Estado do Amazonas (UEA), Manaus, Brazil.
7. IRD, Géoscience Environnement Toulouse (GET-CNRS, IRD, Université de Toulouse), Toulouse, France.
8. LMD, Institut Pierre Simon Laplace (IPSL), Sorbonne Université, Paris, France.
9. Irstea, UR RiverLy, Centre de Lyon-Villeurbanne, Villeurbanne, France
10. Serviço Geológico do Brasil (CPRM), Manaus, Brazil.

\*Corresponding author. Tel: +51 914 116 886. E-mail: armijos.elisa@gmail.com

### Abstract

The biodiversity and productivity of the Amazon floodplain depend on nutrients and organic matter transported with suspended sediments. Nevertheless, there are still fundamental unknowns about how hydrological and rainfall variability influence sediment flux in the Amazon River. To address this gap, we analyzed 3069 sediment samples collected every 10 days during 1995-2014 at five gauging stations located in the main rivers. We have two distinct fractions of suspended sediments, fine (clay and silt) and coarse (sand), which followed contrasting seasonal and long-term patterns. By taking these dynamics into account, it was estimated, for first time, in the Amazon plain, that the suspended sediment flux separately measured approximately 60% fine and 40% coarse sediment. We find that the fine suspended sediments flux is linked to rainfall and higher coarse suspended sediment flux is related with discharge. Additionally this work presents the time lag between rainfall and discharge, which is related to the upstream area of the gauging. This result is an important contribution to knowledge of biological and geomorphological issues in Amazon basin.

### Keywords

Suspended sediment flux, Amazon River, silt, sand, rainfall, discharge, empirical model

## 1. Introduction

The Amazon River accounts for almost one-fifth of global freshwater discharge (Callède et al 2010) and supplies 40% of the Atlantic Ocean's sediment flux (Milliman and Farnsworth 2011). Water and sediment flowing through the Amazon carry carbon and nutrients that fuel productivity on the immense Amazon floodplain, resulting in globally relevant fluxes in organic carbon (Moreira-Turcq et al 2003), water vapor (Salati and Vose 1984), and CO<sub>2</sub> (Abril et al 2013).

The Amazon basin is therefore a critical and strategic zone for studying the effects of climate change and direct human disturbance on water, sediment, and biogeochemical fluxes. Richey et al (1989) showed the importance of climate variability against to human activity. However, the expansion of hydropower and agriculture have recently modified Amazon's land surface processes (Fosberg et al 2017, Latrubresse et al 2017, Anderson et al 2018), which raises questions and concerns about their impacts on discharge and sediment flux alteration in the Amazon River (e.g. Davidson et al 2012; Ferreira et al 2014; Nobre et al 2016). Data and modeling tools are urgently required to anticipate possible consequences of the evolution of climate and anthropological forcing.

The CAMREX project worked on the Amazon plain and estimated annual sediment flux based on the daily variation of water surface slope (Meade et al 1985). Since 1995, the Environmental Research Observatory (SO-Hybam) and national institutes from the Amazon basin have been working together to build a discharge and suspended sediments dataset to understand the dynamics of water and sediment fluxes in different parts of the Amazon basin. the sediment flux was also estimated through indirect methods, such as turbidity and MODIS images (Armijos et al 2017; Espinoza-Villar 2013, 2018, Dos Santos et al 2018), or by using the spatial and temporal variation of gravitational fields from GRACE satellite data (Mouyen et al 2018).

Because of its large size, the daily discharge in the Amazon basin has been estimated by distributed hydrological models such as the MGB-IPH "Modelo de Grandes Bacias", developed by Collichon (2007) and enhanced by De Paiva (2013) and Pontes et al (2015). This model simulates all stages of the hydrological response for different units. Nevertheless, discharge prediction is uncertain at the monthly level because of the seasonality of surface water and groundwater states. Another source of uncertainty is data quality at various spatial and temporal scales (Correa et al 2017). The empirical

1  
2  
3 model based on the historical relationship between inputs (rainfall) and outputs  
4 (discharge) can be used to predict discharge and sediment fluxes in the Amazon River.  
5 For example, Cohen et al (2014) used empirical relationships as an input in a numerical  
6 model to estimate the discharge and sediment flux of the Madeira River, and obtained  
7 robust results. They noted that the temporal variability of precipitation might have a  
8 major effect on water discharge and sediment dynamics. However, the authors used a  
9 short database on sediment flux to validate the model. The use of empirical  
10 relationships requires a large and suitable dataset to catch significant statistical trends.  
11 Setting up such a dataset is one of the main goals of the SO-HYBAM because this  
12 method is not used for the Amazon basin.  
13  
14  
15  
16  
17  
18  
19  
20

21 The relationship between inter-annual rainfall and the concentration of suspended  
22 sediments in the Amazon plain is currently mostly unknown. Several studies based on  
23 different databases propose various main control factors for the annual denudation rate  
24 in the Andes including climate variability, lithology and topographic slope (Pepin et al  
25 2013, Aalto et al 2006). Other studies are inconclusive about the factors that control the  
26 denudation rate in the Andes (Latrubesse and Restrepo 2014).  
27  
28  
29  
30  
31  
32

33 The monthly average concentration at the outlet of the Andean basins in Bolivia and  
34 Peru shows a direct linear rating curve with discharge (Guyot et al 1996, Armijos et al  
35 2013). This relationship shows counter-clockwise hysteresis in the Amazon plain,  
36 which means that the total suspended sediment concentrations are higher during the  
37 rising limb of the hydrograph than at the equivalent water discharge during the falling  
38 period (Richey et al 1986, Dunne et al 1998; Maurice et al 2007). The counter-  
39 clockwise hysteresis is the result of temporal variation in sediment and water discharge  
40 relative to availability due to depletion of available sediment in the basin or in the  
41 stream channel supply (Picouet et al 2001; Walling and Webb 1982).  
42  
43  
44  
45  
46  
47

48 Due to the lack of simple and well-defined empirical relationships, there is no suitable  
49 empirical model to predict monthly or annual sediment flux variation with rainfall or  
50 discharge inputs.  
51  
52  
53  
54

55 The Amazon River and its tributaries transport two well defined suspended sediment  
56 size fractions, which have different dynamics related to rainfall and discharge (Armijos  
57 et al 2017; Dunne et al 1998). Mertes and Meade (1985) showed that the bed forms are  
58  
59  
60

1  
2  
3 composed of dunes by 2 to 5 m in the Amazon River at Óbidos, and the particle size is  
4 between 125 to 500  $\mu\text{m}$  in the Amazon River and its tributaries. Bouchez et al (2011)  
5 compare the relative fine and coarse sediment concentration during the flood period at  
6 Solimões and the Amazon River. Based on this observation, this study propos an  
7 original empirical approach for calculating the sediment flux in the Amazon plain based  
8 on the sediment concentration dynamics of each size fraction: fine [ $C_f$ ] and coarse [ $C_c$ ]  
9 sediment. We analyzed a database of more than 20 years of regular suspended sediment  
10 sampling, where direct empirical relationships can be established between rainfall,  
11 water discharge, [ $C_f$ ] and [ $C_c$ ] for the main tributaries in the Amazon basin. These  
12 relationships reflect the current hydrologic condition in Amazon basin and show the  
13 impacat of rainfall on the water and sediment flux at a monthly step where the transfer's  
14 processes are better reproducibile in a basin of this size. Finally, this relationship is a the  
15 basis for determining the change in sediment production from natural to anthropogenic  
16 influence.

## 27 2. Data and Methods

### 28 2.1 Study Area

29  
30 The Amazon basin an area that is drains  $5.9 \times 10^6 \text{ km}^2$  and includes regions with  
31 contrasting topography, climate and hydrology (Callède et al 2010; Espinoza et al  
32 2009a, b). The Amazon River has an average flow of  $210 \times 10^3 \text{ m}^3 \text{ s}^{-1}$  to the Atlantic  
33 Ocean (Callède et al 2010). As the Amazon approaches the ocean, it receives influx  
34 from the Peruvian, Colombian and Ecuadorian Andes in the Solimões River (60% of  
35 annual average water discharge contribution), from the Peruvian and Bolivian Andes in  
36 the Madeira River (15% of water discharge contribution), and from the Guyana shield in  
37 the Negro River (14% of water discharge). The Solimões and Madeira rivers are rich in  
38 suspended sediment, while the Negro River is largely sediment-free (Filizola and Guyot  
39 2009).

40  
41 This study considers six gauging stations located in the Peruvian and Brazilian plains,  
42 with a long historical data set and contrasts in the seasonality of suspended sediment  
43 concentration and rainfall. The Tamshiyacu gauging station (TAM) is located on the  
44 Amazon River in Peru, below the confluence of the Ucayali and Marañón rivers. In  
45 Brazil, the Manacapuru (MAN) gauging station is located on the Solimões River  
46 upstream of the confluence with the Negro River. There are two gauging stations on the  
47 Madeira River: the Porto Velho (PTV), that is located downstream from the border  
48  
49  
50  
51  
52  
53  
54  
55  
56  
57  
58  
59  
60

1  
2  
3 between Bolivia and Brazil, and the Fazenda Vista Alegre gauging station (FVA),  
4 located in the Madeira River upstream of the confluence with the Amazon River. On the  
5 Branco River, the Caracarai (CAR) gauging station is located upstream of the  
6 confluence with the Negro River, and the Óbidos (OBI) gauging station is located 870  
7 km upstream of the mouth (Figure 1).  
8  
9  
10  
11  
12

## 13 2.2 Data on discharge, rainfall and sedimentology

14  
15 This study used discharge and suspended sediment data provided by SO HYBAM  
16 available at <http://www.ore-hybam.org/>. Discharge was measured with a Rio Grande  
17 600 kHz RDI Acoustic Doppler Current Profiler (ADCP) with a global positioning  
18 system (GPS). Field water discharge in each gauging station was performed regularly,  
19 usually three and four times in the year. For the Tamshiyacu, Caracarai, and Porto  
20 Velho gauging station, we used the rating curve between the level of the river and water  
21 discharge. The Manning-Strickler equation was used to calculate daily discharge in the  
22 Manacapuru, Fazenda Vista Alegre, and Óbidos gauging stations, where there is no  
23 direct relationship due to backwater (Meade et al 1991, Vauchel et al 2017).  
24  
25  
26  
27  
28  
29  
30  
31  
32

33 Rainfall data was gathered from the merged Climate Hazards Group Infrared  
34 Precipitation (CHIRPS) dataset. CHIRPS uses the global cold cloud duration as a  
35 primary source to calculate global precipitation. This initial estimation is then calibrated  
36 with the precipitation product from TRMM-3B42 V7 and information from the global  
37 rain gauge network, resulting in a high spatial resolution rainfall data set ( $0.25^{\circ} \times 0.25^{\circ}$ ).  
38 Satellite data provide daily and monthly precipitation data sets from January 1981 to  
39 December 2017 (Funk et al 2015). CHIRPS data has been compared previously with  
40 data from observation-based rainfall products and from a meteorological station in the  
41 Amazon basin (Espinoza et al 2019).  
42  
43  
44  
45  
46  
47  
48  
49

50 SO HYBAM has been monitoring discharge and suspended sediment concentration in  
51 Brazil since 1995 and Peru since 2003. The suspended sediment data set has a total of  
52 3069 surface measurements taken every 10 days and 113 discrete cross-section  
53 measurements taken during different periods of the annual hydrological regime from  
54 2003 to 2014 (e.g., Óbidos gauging station, Figure 1b). A similar sampling protocol was  
55 used by the SO-HYBAM observatory. Discrete water samples (5 L or 7 L) were  
56  
57  
58  
59  
60

1  
2  
3 collected at different depths for several profiles with samples less than 1 m from the  
4 riverbed. The spatial location of the profiles in the cross section depends was  
5 determined with equal discharge. For each sample, the coarse and fine sediments are  
6 separated using a 63  $\mu\text{m}$  sieve. A 400 mL sample of the fine sediments was filtered  
7 through a 0.45  $\mu\text{m}$  cellulose filter. Repeated measurements revealed an uncertainty of  
8 10% for surface concentrations and 25% for the concentrations near the river bottom.  
9  
10 The data for both the discharge and the suspended sediments are stored and processed  
11 with Hydraccess software ([http://www.ore-](http://www.orehybam.org/index.php/eng/software/Hydraccess)  
12 [hybam.org/index.php/eng/software/Hydraccess](http://www.orehybam.org/index.php/eng/software/Hydraccess)). Details of the field measurements are  
13 described in Armijos et al (2017) and Vauchel et al (2017).  
14  
15  
16  
17  
18  
19  
20  
21

22 Analysis of suspended sediment concentration therefore considers two fractions:  
23 particles  $>0.45 \mu\text{m}$  and  $<63\mu\text{m}$  ( $[Cf]$ ) and particles  $>63 \mu\text{m}$  ( $[Cc]$ ). The  $[Cf]$  and  $[Cc]$   
24 have very different seasonal signals during the hydrological year. At OBI, for example,  
25 the  $[Cf]$  peak occurs between February and March, during the rainy period, and the  $[Cc]$   
26 peak between April and June, during the flood period (Figure 1 c, d).  
27  
28  
29  
30  
31  
32  
33  
34  
35  
36  
37  
38  
39  
40  
41  
42  
43  
44  
45  
46  
47  
48  
49  
50  
51  
52  
53  
54  
55  
56  
57  
58  
59  
60



1  
2  
3  
4 Figure 1. a) The Amazon basin and location of gauging stations: Tamshiyacu (TAM) on the Amazon River, Manacapuru (MAN) on the Solimões  
5 River, Caracarai (CAR) on the Branco River, Porto Velho (PTV) and Fazenda Vista Alegre (FVA) on the Madeira River, and Óbidos (OBI) on  
6 the Amazon River. b) Temporal records of the measured suspended sediments load at the Óbidos gauging station: green diamond = ALPHA  
7 HELIX project (1976-1977); brown diamond = CAMREX project (1982-1984), measurements used by Meade et al (1985). White circles are  
8 surface suspended sediments and red squares are suspended sediments' discrete cross-section measurements = SO-HYBAM observatory (1995-  
9 2015), c) Mean monthly rainfall in the Amazon basin at the Óbidos gauging station (CHIRPS dataset (1981-2017), and mean monthly water  
10 discharge of Amazon basin at the Óbidos gauging station (1981-2016), d) Temporal suspended sediment concentration of  $[C_f]$  and  $[C_c]$  at  
11 Óbidos station.  
12  
13  
14  
15  
16  
17  
18  
19  
20  
21  
22  
23  
24  
25  
26  
27  
28  
29  
30  
31  
32  
33  
34  
35  
36  
37  
38  
39  
40  
41  
42  
43  
44  
45  
46

### 2.3 Discharge, rainfall and sediment relationships

There are significant time lags between rainfall input and water discharge response because of the large size of the Amazon basin. Several methods can be applied to calculate basin time lag between rainfall and discharge (Granato 2012). This time lag depends on control factor patterns, such as basin soil wetness, the nature of flow paths, and rainfall distribution. However, this information is limited or has large uncertainties in the Amazon basin. For this study, the rainfall-discharge time lag was defined with a cross-correlation analysis for the daily level of the average basin-integrated rainfall for each of the six basins and their respective discharge. The mean climatological annual cycle of both series is removed to eliminate seasonality.

The lag times and the Hack law (Hack 1957), can also derive an average travel velocity ( $V$ ) of the water over the drainage area ( $A$ ) for each basin as follows:

$$V = L/t \quad (1)$$

Here,  $L$  is the characteristic basin length, and  $t$  is the lag time between rainfall and discharge.  $L$  is obtained from the Hack law, which defines the longest upstream length with the drainage area ( $A$ ) at a specific point of the drainage network:

$$L = A^{0.56} \quad (\text{see Supplementary Material for more detail about the Hack's law})$$

Armijos et al (2017) observe an increase [ $Cc$ ] during the flood period, and they concluded that the capacity of the Amazon River and tributaries increase during this period. This observation suggests an empirical relationship between [ $Cc$ ] and discharge. However, we considered the river bed shear stress instead of the water discharge only.

$$[Cc] = au^{*b} \quad (2)$$

To evaluate the river bed shear stress, we used stage-discharge-rating curves to estimate hydraulic parameters with  $a$  and  $b$  fitting coefficients for section-averaged flow velocity and hydraulic radius (Camenen et al 2014).

We also explored the related hydro-sedimentary model to discuss the potential use of a sediment transport capacity (Camenen and Larson 2008) to predict the sand suspended load. The supplementary material summarizes the methodology and the data that have been used as input to the Camenen et al (2014)'s model including, particle sizes, cross-section at gauging stations and discharge datasets.

Eventually, we also studied the monthly relationship between rainfall and fine suspended sediment flux ( $Q_{sf}$ ) with  $a$  and  $b$  fitting coefficients.

$$Q_{sf} = aR^b \quad (3)$$

### 3. Results

#### 3.1 Rainfall and discharge Relationship.

The counter-clockwise hysteresis between rainfall and discharge shows the response time between the maximum peak rainfall in the basin and the maximum draining away to the main river at OBI. We found that the maximum peak rainfall is between January and March, and the maximum peak of discharge is between May and June. The counter-clockwise hysteresis is reproducible every year, which implies that the same rising and falling events occur during the same periods each year. This produces a reliable lag time for the entire OBI dataset (Figure 2a). The same trend is observed at the other gauging stations, with different lag times between rainfall in all basins and discharge peaks.

The lag time is 102 days, with  $r^2 = 0.98$  at OBI for the period 1981 to 2016 (Figure 2b). The supplementary materials summarize the lag values for each gauging station. Using the same procedure, lag times for the other gauging stations were calculated for the same period as for OBI (Figure 2 c-g). The monthly rainfall and discharge relationships do not show any hysteresis and follow simple linear trends with coefficient of determination values between 0.95 and 0.99 on a monthly scale, if we take into account the respective time lag at each station (Table 1). These empirical relationships could be used to determine monthly discharge at each station when the amount of rainfall in the basin is known.

1  
2  
3 The monthly discharge was calculated using the empirical relationship of rainfall to  
4 discharge and has an RMSE of <11% for the Madeira and Solimões rivers and <14% for  
5 the Amazon and Branco rivers, in comparison with the field observations.  
6  
7  
8  
9

10 The scaling of lag times via the upstream length of the river at each station, converge to  
11 similar values of water transit velocity  $V \sim 38$  km/day  $\pm 10\%$  (Óbidos value of  $V$  not  
12 included – Table 1, Supplementary Material). This is over a large part of the Amazon  
13 plain and a large range of geological contexts, including the sub-basins of different  
14 orders of magnitude, water discharges, and sediment concentrations. The larger  $V$   
15 observed at OBI indicates a decrease in the average water velocity. We did not currently  
16 push the analysis further to better understand this downstream shift of  $V$ . It may be  
17 related to the channel-flood plain connection in this area that was already described in  
18 previous studies (Dunne, 1998).  
19  
20  
21  
22  
23  
24  
25  
26

27 Our study shows that the monthly discharge of the Amazon River network can be  
28 deduced via the effective rainfall rate for the specific location and applying  $V \approx 38$  km  
29 day<sup>-1</sup> for the time lag calculation. Note that there is no need to apply a correction factor  
30 suggesting that there is no notable variability in the average rainfall efficiency rate in  
31 the Amazon plain.  
32  
33  
34  
35  
36  
37  
38  
39  
40  
41  
42  
43  
44  
45  
46  
47  
48  
49  
50  
51  
52  
53  
54  
55  
56  
57  
58  
59  
60

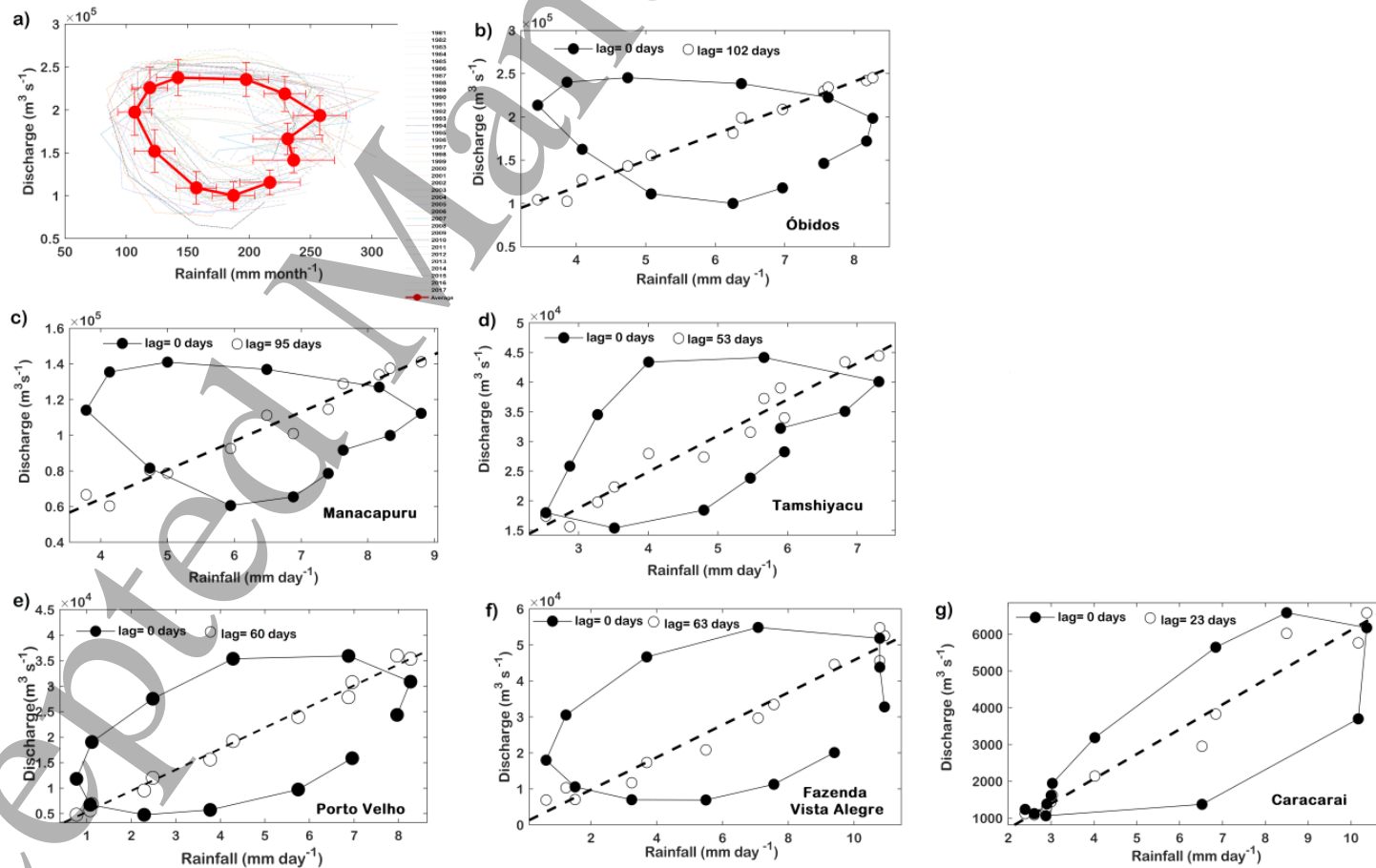


Figure 2. a) Rainfall ( $\text{mm month}^{-1}$ ) vs discharge ( $\text{mm month}^{-1}$ ) for the 1981-2016 period, gray = annual trend, red = inter-annual averaged data; 2b), 2c), 2d), 2e), 2f), and 2g) are inter-annual monthly averaged data for Obidos, Manacapuru, Tamshiyacu, Porto Velho, Fazenda and Caracarai gauging stations, respectively. Black dots are monthly averaged data with no time lag. White dots are monthly averaged data with the time lag between rainfall and discharge. See Supplementary Material for time lag calculation explanation

### 3.2 Relationship between discharge and coarse suspended sediment concentration $[Cc]$ .

$[Cc]$  in the Amazon basin increases during the flood period in the Amazon main stream between Tamshiyacu and Óbidos (Armijos et al 2017). Higher local discharge induces re-suspension of coarse particles from the riverbed and greater hydraulic capacity of river transport. By analyzing the field measurements of  $[Cc]$  and discharges, we found that both variables are related via a power law that is specific for each station. The strong correlation between  $[Cc]$  and discharge allow us to calculate the coarse suspended sediment flux using the empirical rating curve (with  $r^2 =$  between 0.57 and 0.89 for all gauging stations). The shear velocity and  $[Cc]$  relationship (Eq.2) present a relatively narrow range of the exponent value between 5 and 6, except for the OBI data. This indicates that a common hydraulic model can be explored and used to obtain a first estimation of  $[Cc]$  for a range of river scales of one order of magnitude in the Amazon plain. The OBI exception is not yet explained and will be explored in the future (Figure 3). Coefficients in the equation of the relationship between  $u^*$  and  $[Cc]$  are seen in Table 1. This relationship is then used to calculate the coarse sediment flux.

In the Supplementary Material (Figure 6), the results of sand sediment flux obtained using a sediment transport capacity are presented based on Camenen et al (2008, 2014). Good agreement is observed between the model and data for all stations except for the OBI with a large overestimation is observed. The results indicates that the sand suspension capacity is reached *a priori*; thus, this result validates the use of an empirical formula for prediction. In the case of OBI, the difference may be explained by the singularity of this station located in a very constrained zone with high velocities. At OBI, the sand concentrations are indeed more regulated by the upstream reach that is larger and less dynamic.

Bedload has been calculated using the Camenen and Larson (2005) formula (see Supplementary Material Figure 6) and this show negligible contribution ( $\approx 1\%$ ) in comparison to suspended load

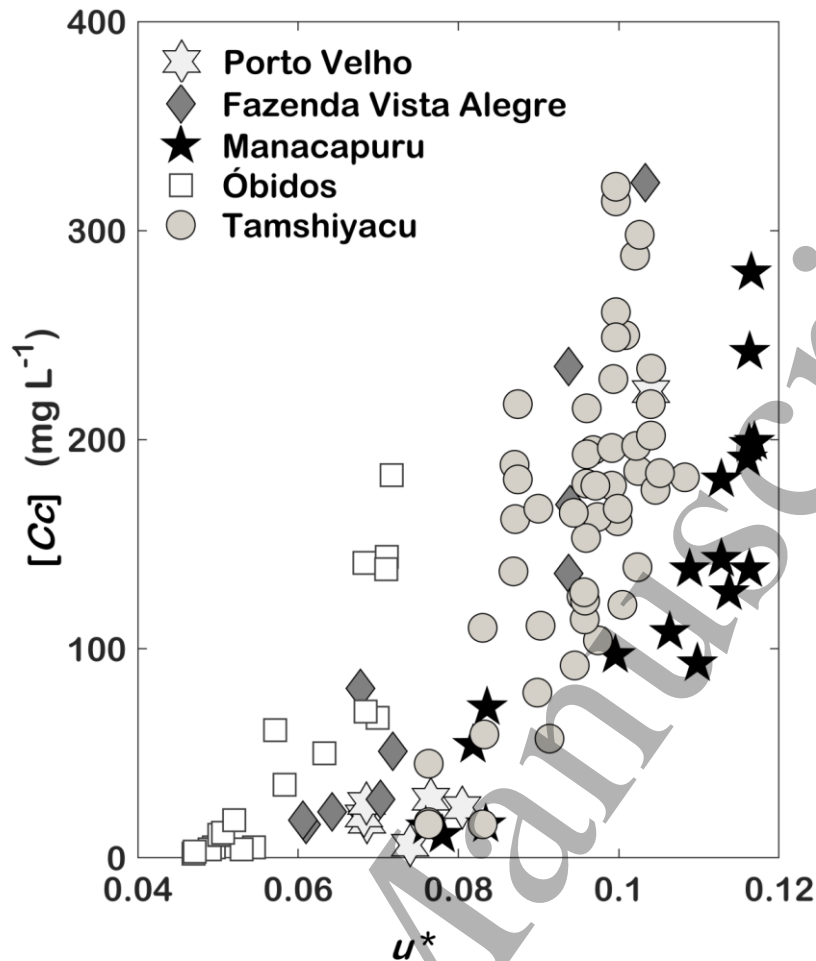


Figure 3. Plot of the measured sand concentration  $[Cc]$  versus shear velocity ( $u^*$ ) for the six gauging stations (1995-2014),  $[Cc] = au^{*b}$ .

### 3.3 Relationship between rainfall and fine suspended sediment flux $Q_{sf}$ .

To establish the relationship between  $Q_{sf}$  and rainfall, we used a dataset of  $[Cf]$  derived from surface sample ( $[Cf]_{surface}$ ) every 10 days via a bottle filled in the middle of the cross-section at each gauging station. Note that  $[Cf]$  represents the average fine suspended sediment at cross-section, and  $[Cf]_{surface}$  data show a well-defined unique linear relationship regardless of the gauging station ( $[Cf] = 1.17 * [Cf]_{surface}$ , Figure 4). This indicates that one sample taken at the surface can be representative of  $[Cf]$  in a cross-section of the Amazon plain.

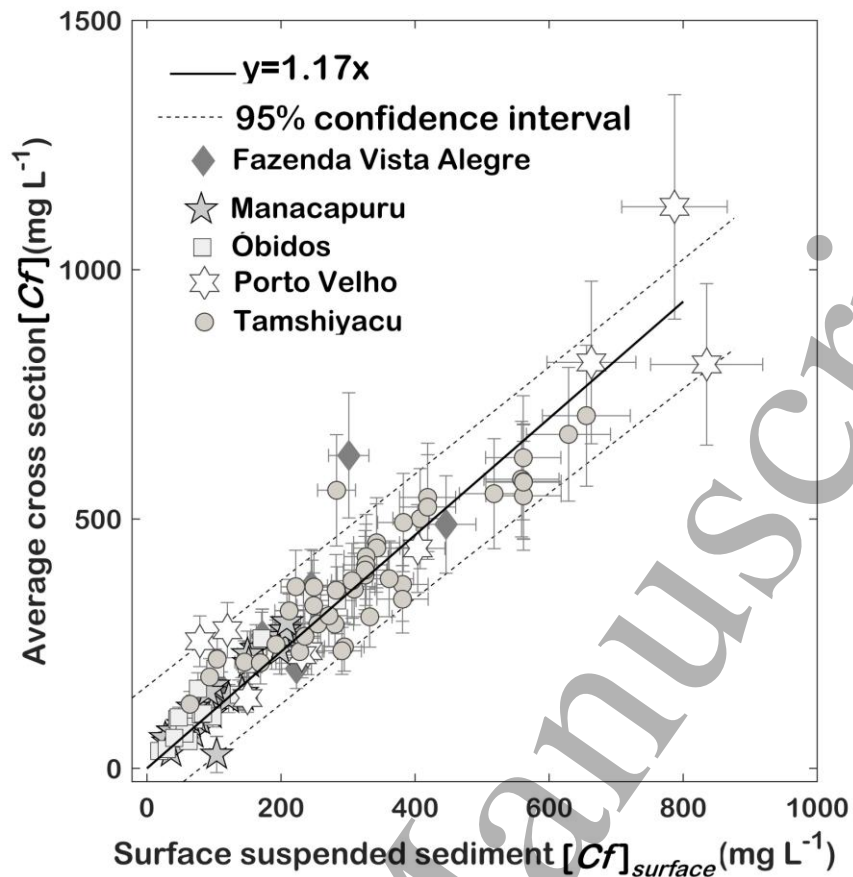


Figure 4. Relationship between fine suspended sediment at the surface ( $[Cf]_{surface}$ ) and average fine suspended sediment concentration over cross-section ( $[Cf]$ ) at six gauging stations

This study shows that there is a power-law relationship between the mean monthly rainfall and fine suspended sediment flux ( $Q_{sf}$ ), with  $r^2 > 0.7$  for all gauging stations in the plain. The narrow range of exponent values is between 1.9 and 2.3, except at the CAR station (1.16) (Table 1). There is a time lag of 1 month between rainfall and  $Q_{sf}$  at OBI, FVA, PTV and CAR, with no time lag at MAN and TAM. Both gauging stations located downstream from the Andean piedmont (TAM and PTV) and show a similar rating curve (Figure 5).

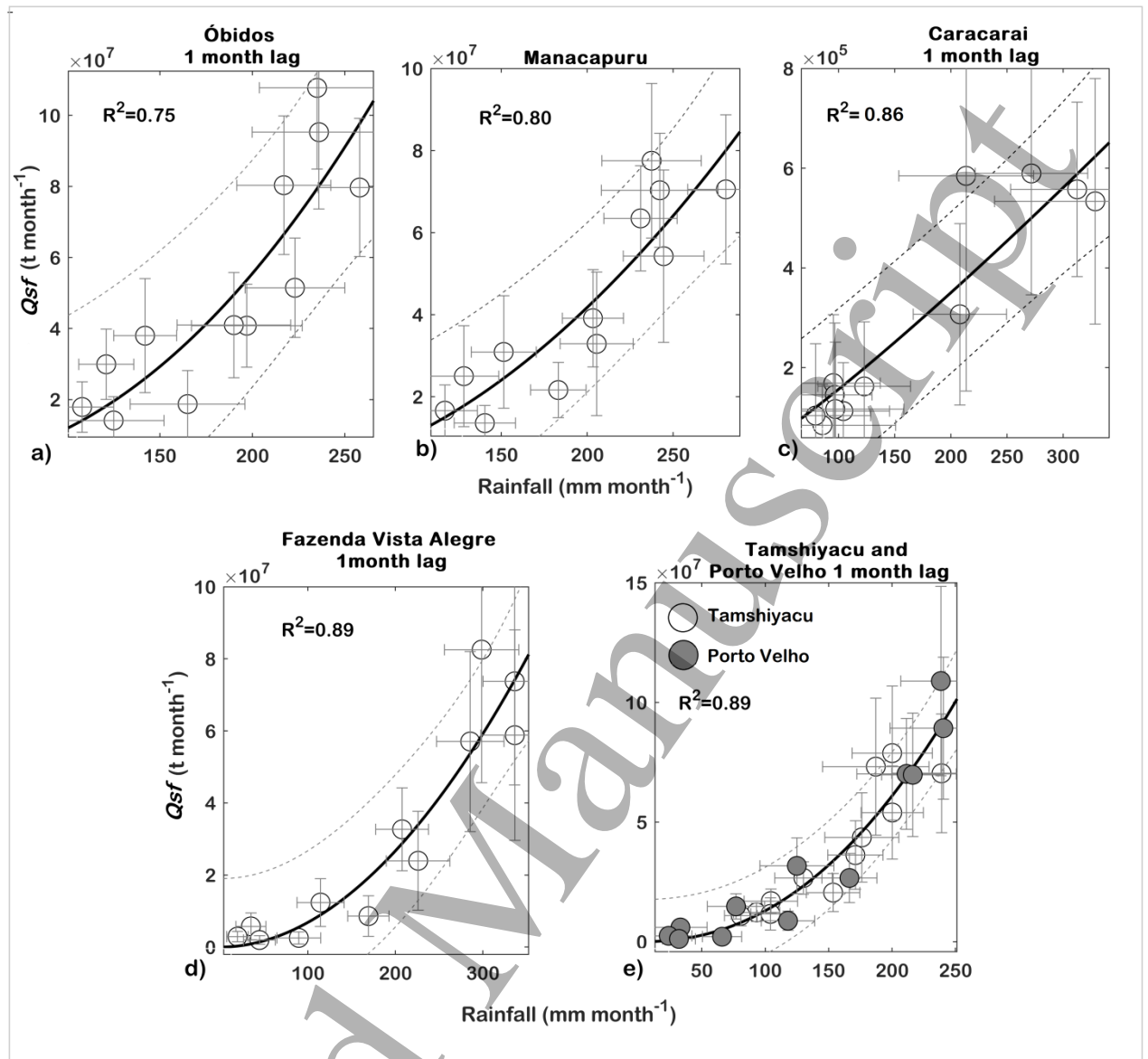


Figure 5. Relationship between rainfall and  $Q_{sf}$ , with 95% confidence interval (dotted line) at the gauging stations of a) Óbidos, b) Manacapuru, and c) Caracarai with a 1-month lag as well as: d) Fazenda Vista Alegre with a 1-month lag, and e) Tamshiyacu with white circle and Porto Velho with a 1-month lag.

Table 1. Time of response (lag time) between rainfall (mm day<sup>-1</sup>) and discharge (m<sup>3</sup> s<sup>-1</sup>), and fitting values for Eqs. 2, and between  $u^*$ (m s<sup>-1</sup>) and  $[Cc]$  (mg L<sup>-1</sup>) and between rainfall (mm month<sup>-1</sup>) and  $Qsf$  (t month<sup>-1</sup>) for six gauging stations respectively.

River	Gauging Station	Rainfall (R) (vs) Discharge (Q)				$u^*$ (vs) $[Cc]$		Rainfall (vs) $Qsf$			
		$Q = aR + b$	$r^2$	Lag time (days)	RMSE %	$[Cc] = au^{*b}$	$r^2$	$Qsf = aR^b$	$r^2$	Lag time (days)	RMSE %
Amazon	Tamshiyacu	$Q = 611 \times R + 422$	0.95	53	29	$[Cc] = 2E + 0.8 \times u^{*6.05}$	0.57	$Qsf = 443 \times R^{2.23}$	0.89	-	30
Solimões	Manacapuru	$Q = 16230 \times R - 630$	0.96	95	5	$[Cc] = 3E + 0.7 \times u^{*5.57}$	0.84	$Qsf = 161 \times R^{1.92}$	0.80	-	23
Madeira	Porto Velho	$Q = 4133 \times R + 1192$	0.99	60	6	$[Cc] = 1E + 0.8 \times u^{*5.74}$	0.65	$Qsf = 443 \times R^{2.23}$	0.89	30	22
Madeira	Fazenda	$Q = 4498 \times R + 771$	0.96	63	11	$[Cc] = 4E + 0.7 \times u^{*5.18}$	0.89	$Qsf = 806 \times R^{2.0}$	0.89	30	30
Branco	Caracarai	$Q = 674.3 \times R - 632$	0.96	23	14			$Qsf = 743 \times R^{1.16}$	0.86	30	34
Amazon	Óbidos	$Q = 30410 \times R - 2521$	0.98	102	13	$[Cc] = 4E + 1.5 \times u^{*11.75}$	0.87	$Qsf = 429 \times R^{2.27}$	0.75	30	34

1  
2  
3  
4  
5 The one-month lag could be due to the heterogeneous spatial distribution of rainfall in  
6 the basin and the different sources of suspended sediments. The interesting question is  
7 why this lag was not observed at the TAM and MAN (Amazon/Solimões) gauging  
8 stations. This should be explained with more specific data in the future; nevertheless,  
9 Espinoza et al. (2012) show that the peak of suspended sediments occurred at the same  
10 time as the peak of rainfall at TAM. All stations, have low uncertainty (RMSE = 30%),  
11 and this implies that  $Q_{sf}$  can be better predicted from rainfall rate in each watershed,  
12 rather than from discharge. This is because there is no complex interpretation of the  
13 hysteresis trend. Rainfall is probably a more significant control factor of  $Q_{sf}$  than  
14 discharge. Note that historical sediments deposited into the Bolivian basin (Aalto et al.  
15 2003) have suggested sensitivity between the fine sediment transport rate and rainfall.  
16  
17  
18  
19  
20  
21  
22  
23  
24  
25

### 26 3.4 Suspended sediment flux

27 It is possible to calculate the sediment flux over the Amazon plain using rainfall data  
28 only from the three relationships shown in the section 3.1, 3.2 and 3.3 (Eq. 2 and 3 with  
29 fitting coefficients presented in Table 1). Estimates of sediment flux using the empirical  
30 relationship described in this study are comparable to values proposed in the literature  
31 considering the range of uncertainties (Eq. 4 Figure 6a).  
32  
33  
34  
35  
36

$$37 Q_s = Q_{sf} + Q_{sc} = Q([C_f] + [C_c]) \quad (4)$$

38  
39  
40  
41 Distinguishing between fine and coarse particles is important because the dynamics of  
42 these two grain-size types of suspended sediments are different during the annual  
43 hydrological regime. A sandy sediment flux is strongly related to local water discharge,  
44 with no limitation of supply. Fine sediment flux is mainly controlled by annual rainfall  
45 distribution (Figure 6 b, c). Thus, the different scales of rainfall distribution and climatic  
46 factors, control the two types of sediment flux in the Amazon basin.  
47  
48  
49  
50  
51  
52  
53  
54  
55  
56  
57  
58  
59  
60

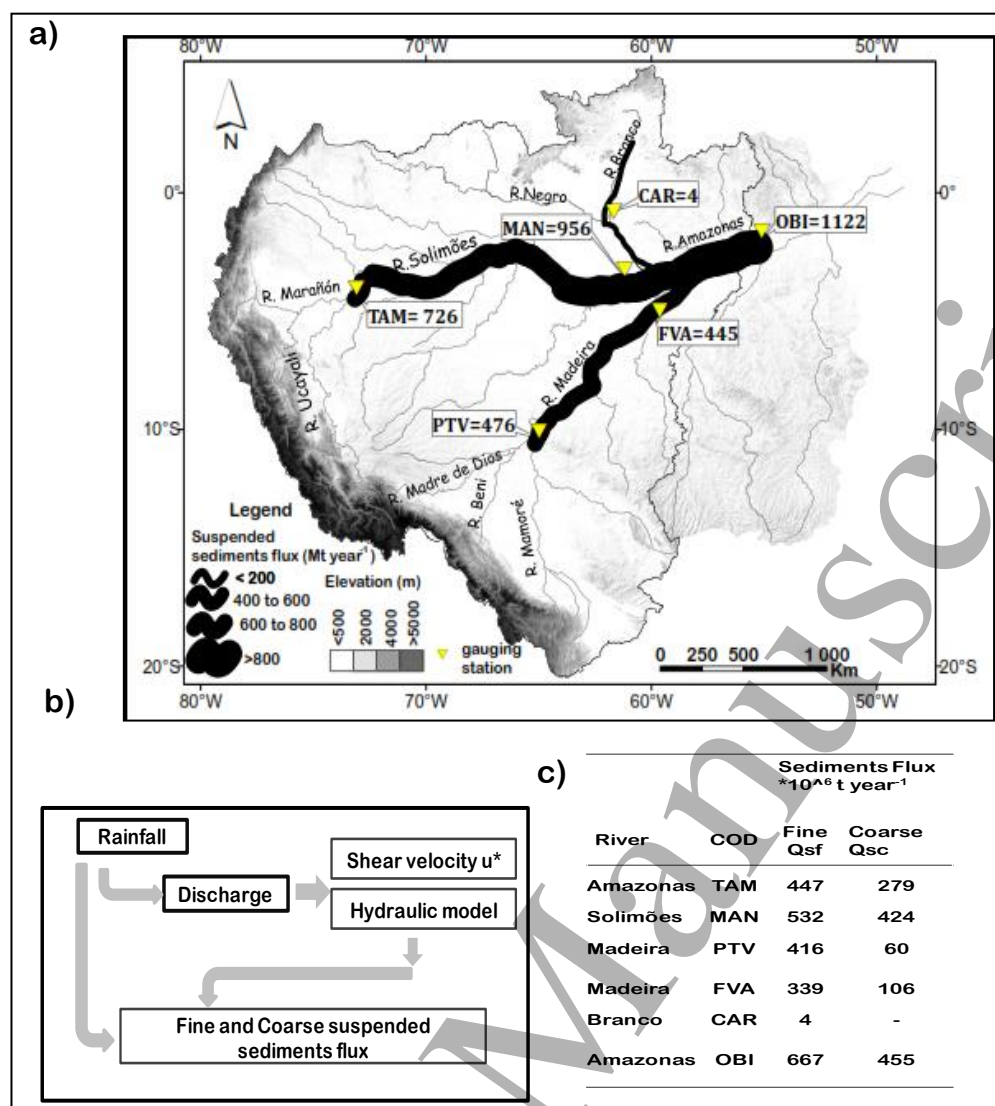


Figure 6. a) Annual sediment flux calculated in this study at the Tamshiyacu, Manacapuru, Porto Velho, Fazenda Vista Alegre, Caracarai, and Óbidos with an RSME of 30%. b) Conceptual diagram of the empirical model for predicting water discharge and sediment flux from rainfall data c) Fine and coarse suspended sediment flux estimate with the empirical relationship.

In summary, rainfall plays an important role in the dynamics of fine and coarse suspended sediments in the Amazon basin, and this influence is differentiated in space and time. Fine sediments are eroded at the beginning of the rainy season in the Andean region, where the peak of  $[C_f]$  is during the wet period. Coarse suspended sediment flux in the Amazon plain is directly related to local water discharge and therefore to the rainfall rate upstream.

1  
2  
3 The empirical model used in this study enables the novel possibility to predict sediment  
4 fluxes in the Amazon River network, considering the actual conditions. In the case of  
5 sand, the model corresponds to a set of sediment transport capacities validated on the  
6 Amazon system. Sands represent 25% to 48% of the annual sediment fluxes in the  
7 Madeira, Solimões and Amazon rivers and do not transit downstream in phase with fine  
8 sediments. This is because fine and coarse sediments are not strictly controlled by the  
9 same factors. This empirical model can estimate how these two types of sediment fluxes  
10 might vary with climatic variability and global land change.  
11  
12  
13  
14  
15  
16  
17  
18  
19  
20

#### 21 4. Conclusions

22 This work analyzed suspended sediment flux in the Amazon plain, considering two  
23 types of suspended sediments (fine and coarse) over 20 years (1995-2014). The  
24 sediments were related to discharge and rainfall.  
25  
26

27 The time lag between rainfall and discharge has been established and is related to the  
28 area upstream of the gauging station. This is a primary concern, because clay, silt and  
29 sand sediments have different impacts on the transport of nutrients or heavy metals,  
30 river geomorphology, biodiversity, fluvial transport, and/or dam projects.  
31  
32

33 Considering the time of concentration in the empirical analysis of the relationship  
34 between rainfall and discharge, a simple linear trend can be applied to calculate mean  
35 monthly discharge for any location in the Amazon plain. Rainfall over the Amazon  
36 plain can be used to directly estimate discharge and fine suspended sediments flux and  
37 to indirectly to estimate sandy sediment flux.  
38  
39  
40  
41  
42  
43  
44

45 This methodology could be explored in other large rivers systems. In the Solimões,  
46 Amazon, Madeira and Branco rivers, the total suspended sediment flux is formed  
47 mainly by fine suspended sediments. However, coarse (sand) sediment flux is not  
48 negligible, especially in the Solimões River, where the contribution for sand comes  
49 from northern tributaries such as the Iça or Japurá rivers (Dunne et al 1998), and it can  
50 reaches close to 50% of the total flux for the Solimões River.  
51  
52  
53  
54

55 The physical model proposed by Camenen et al (2008, 2014) is relevant because it is  
56 based on a large data set including field data. The data show robustness to predict the  
57  
58  
59  
60

sands flux (apart for the OBI station). The values indicated that sediment transport capacity is achieved for all stations.

Using this empirical model, we can predict discharge and sediment flux under different climatic conditions that control rainfall input over the Amazon basin. These values could be applied for prediction considering that the current surface condition of the basin does not change too much. Any change in this empirical set of trends leading to hydrologic response in the atmospheric input could be used to establish several changes of natural or anthropogenic impacts if any of the statistics change.

### Acknowledgements

The authors thank Thomas Dunne and the anonymous reviewers for their comments and observations, which helped us to improved this work. We also thank the Observation Service for the Geodynamical, Hydrological and Biogeochemical Control of Erosion/Alteration and Material Transport in the Amazon Basin (SO-HYBAM) and the National Water Agency (ANA), the Geological Survey of Brazil (CPRM), and the IHESA project for support during field campaigns. We also thank Bosco Alfenas and Chuck Goll. We thank the National Institute of Amazonian Research (INPA), the University of the State of Amazonas (UEA), and the Climate and Environmental Program (CLIAMB), especially Dr. Luis Cândido and Dr. Rita Valeria Andreoli. We also thank the PNICP-Peru through the 'N°397-PNICP-PIAP-2014' contract.

### 5. References

- Aalto R, Maurice-Bourgoin L, Dunne T, Montgomery D R, Nittrouer, C A, Guyot J L 2003 Episodic sediment accumulation on Amazonian flood plains influenced by El Nino/Southern Oscillation. *Nature*. **425** 493-497.
- Aalto R, Dunne T, Guyot J L 2006. Geomorphic controls on Andean denudation rates. *J. Geol.* **114** 85–99.
- Abril G, Martinez JM, Artigas L F, Moreira-Turcq P, Benedetti M F, Vidal L, Meziane T, Kim JH, Bernardes M C, Savoye N, Deborde J, Lima Souza E, Albéric P, De Souza M, and Roldan F, 2013 Amazon River carbon dioxide outgassing fuelled by wetlands *Nature*. **505** 395-398.
- Anderson E P, Jenkins C N, Heilpern S, Maldonado-Ocampo J A, Carvajal-Vallejos F M, Encalada A C, Salcedo N 2018 Fragmentation of Andes-to-Amazon connectivity by hydropower dams *Sci. Adv.* **41** 1642.
- Armijos E, Crave A, Vauchel P, Fraizy P, Santini W, Moquet J S, Arevalo N, Carranza J, Guyot J L 2013 Suspended sediment dynamics in the Amazon River of Peru *J. South. Am. Earth. Sci.* **44** 75-84.

- 1  
2  
3 Armijos E, Crave A, Espinoza R, Fraizy P, Dos Santos A L M R, Sampaio F, Pantoja  
4 N 2017 Measuring and modeling vertical gradients in suspended sediments in the  
5 Solimões/Amazon River *Hydrol. Process.* **313** 654-667.
- 6 Bouchez J, Métivier F, Lupker M, Maurice L, Perez M, Gaillardet J, France Lanord C  
7 2011 Prediction of depth integrated fluxes of suspended sediment in the Amazon  
8 River: Particle aggregation as a complicating factor. *Hydrol. Process.* **5** 778-794.
- 9 Callède J, Cochonneau G, Alves F V, Guyot JL, Guirimães V S, De Oliveira E, 2010  
10 Les apports en eau de l'Amazone à l'Océan Atlantique *J. Water Sci.* **233** 247-273.
- 11 Camenen B and Larson M 2005 A bedload sediment transport formula for the nearshore  
12 *Estuar. Coast. Shelf. Sci.* **63** 249-260.
- 13 Camenen B and Larson M 2008 A general formula for non cohesive suspended  
14 sediment transport *J. Coast. Res.* **24** 615-627.
- 15 Camenen B, Le Coz J, Dramais G, Peteuil C, Fretaud T, Falgon A, Moore S A 2014 A  
16 simple physically-based model for predicting sand transport dynamics in the  
17 Lower Mekong River *Proc. River Flow Conf.* Lausanne Switzerland.
- 18 Cohen S, Kettner A J, Syvitski, J P 2014 Global suspended sediment and water  
19 discharge dynamics between 1960 and 2010: Continental trends and intra-basin  
20 sensitivity. *Glob. Plan. change.* **115** 44-58.
- 21 Collischonn W, Allasia D, Da Silva B C, Tucci C E 2007 The MGB-IPH model for  
22 large-scale rainfall—runoff modelling *J. Hydrol. Sci. J* **525** 878-895.
- 23 Correa S W, de Paiva R C, D Espinoza J C, Collischonn W 2017 Multi-decadal  
24 Hydrological Retrospective: Case study of Amazon floods and droughts *J Hydrol.*  
25 **549** 667-684.
- 26 Davidson E A, de Araújo A C, Artaxo P, Balch J K, Brown I F, Bustamante M, Coe M,  
27 De Fries R, Keller M, Longo M, Munger W, Schroeder W, Soares-Filho B, Souza  
28 Jr C, Wofsy S 2012 The Amazon basin in transition *Nature.* **481** 321-328.
- 29 De Paiva R C, Buarque D C, Collischonn W, Bonnet M P, Frappart F, Calmant S,  
30 Bulhoes C A 2013 Large-scale hydrologic and hydrodynamic modeling of the  
31 Amazon River basin *Water. Resour. Res.* **493** 1226-1243.
- 32 Dos Santos A L M R, Martinez J M, Filizola Jr N P, Armijos E, Alves L G S 2018  
33 Purus River suspended sediment variability and contributions to the Amazon  
34 River from satellite data 2000–2015 *Comp. Rend. Geosc.* **350** 13-19.
- 35 Dunne T, Mertes L A, Meade R H, Richey J E, Forsberg B R 1998 Exchanges of  
36 sediment between the flood plain and channel of the Amazon River in Brazil  
37 *Geolog. Societ. Amer. Bulletin.* **1104** 450-467.
- 38 Espinoza J C, Ronchail J, Guyot J L, Cochonneau G, Naziano F, Lavado W, Vauchel P  
39 2009a Spatio-temporal rainfall variability in the Amazon basin countries Brazil  
40 Peru Bolivia Colombia and Ecuador *Int. J. Climatol.* **2911** 1574-1594.
- 41 Espinoza J C, Guyot J L, Ronchail J, Cochonneau G, Filizola N, Fraizy P, Labat D, de  
42 Oliveira E, Ordoñez J, Vauchel P 2009b Contrasting regional discharge evolutions  
43 in the Amazon Basin 1974-2004 *J Hydrol.* **375** 297-311.
- 44 Espinoza J C, Ronchail J, Marengo J A, Segura H 2019 Contrasting North–South  
45 changes in Amazon wet-day and dry-day frequency and related atmospheric  
46 features 1981–2017 *Clim. Dyn.* **52** 5413–5430.
- 47 Espinoza Villar R, Martinez J M, Le Texier M, Guyot J L, Fraizy P, Meneses P R,  
48 Oliveira E 2013 A study of sediment transport in the Madeira River Brazil using  
49 MODIS remote-sensing images *J. South Americ Earth Sci* **44** 45-54.
- 50 Espinoza-Villar R, Martinez J M, Armijos E, Espinoza J C, Filizola N, Dos Santos A,  
51 Willems B, Fraizy P, Santini W, Vauchel P 2018 Spatio-temporal monitoring of  
52  
53  
54  
55  
56  
57  
58  
59  
60

- suspended sediments in the Solimões River 2000–2014 *Compt. Rend. Geosci.* **3501** 4-12.
- Ferreira J, Aragão L, Barlow J, Barreto P, Berenguer E, Bustamante M, Gardner T, Lees A, Lima A, Louzada J, Pardini R, Parry L, Perees C A, Pompeu P S, Tabarelli M, Zuanon J 2014 Brazil's environmental leadership at risk *Sci* **346** 706–707.
- Filizola N and Guyot J L 2009 Suspended sediment yields in the Amazon basin: an assessment using the Brazilian national data set *Hydrol. Process.* **2322** 3207-3215
- Filizola N, Guyot J L, Wittmann H, Martinez J M, de Oliveira E 2011 The significance of suspended sediment transport determination on the Amazonian hydrological scenario *Sedimen. transport in aquatic environm.*
- Forsberg B, Melack J, Dunne T, Barthem R, Goulding M, Paiva R C, Sorribas M, Silva U, Weisser S 2017 The potential impact of new Andean dams on Amazon fluvial ecosystems *PloS One* **128** e0182254.
- Funk C, Peterson P, Landsfeld M, Pedreros D, Verdin J, Shukla S, Husak G, Rowland J, Harrison L, Hoell A, Michaelsen J 2015 The climate hazards infrared precipitation with stations—a new environmental record for monitoring extremes *Sci. Data* **2** 150066.
- Granato G E 2012 Estimating basin lagtime and hydrograph-timing indexes used to characterize storm flows for runoff-quality analysis *Scientif. Investigat. Report.*
- Guyot J L, Fillzola N, Quintanilla J, Cortez J 1996 Dissolved solids and suspended sediment yields in the Rio Madeira basin from the Bolivian Andes to the Amazon *Proceeding of the Exeter Symposium IAHS public* 55-64.
- Guyot J L, Bazan H, Fraizy P, Ordonez J, Armijos E, Laraque A 2007 Suspended sediment yields in the Amazon basin of Peru: a first estimation *IAHS public*.
- Hack J T 1957 Studies of longitudinal stream profiles in Virginia and Maryland. US Governemt *Printing Office*. Paper B **294** 1-97.
- Latrubesse E, Arima E, Dunne T, Park E, Baker V R, d'Horta F M , Wight C, Wittmann F, Zuanon J, Baker P, Ribas C, Norgaard R, Filizola N, Ansar A, Flyvbjerg B, Stevaux J 2017 Damming the rivers of the Amazon basin *Nature*. **546** 363-369.
- Latrubesse E M and Restrepo J D 2014 Sediment yield along the Andes: continental budget regional variations and comparisons with other basins from orogenic mountain belts *Geomorphology*. **216** 225-233.
- Maurice L, Bonnet M P, Martinez J M, Kosuth P, Cochonneau G, Moreira-Turcq P, Seyler P 2007 Temporal dynamics of water and sediment exchanges between the Curuaí floodplain and the Amazon River Brazil *J. Hydrol.* **335** 140-156.
- Meade R H 1985 Suspended sediment in the Amazon River and its tributaries in Brazil during 1982-84 *US Geol. Survey*.
- Meade R H, Rayol J M, Da Conceição S C, Natividade, J R 1991 Backwater effects in the Amazon River basin of Brazil *Environ. Geol. and Water Sci* **18** 105-114.
- Mertes, L A, and Meade, R H 1985. Particle sizes of sands collected from the bed of the Amazon River and its tributaries in Brazil during 1982-84. 85-333. *US Geol. Survey*.
- Milliman J D and Farnsworth K L 2011 River discharge to the coastal ocean: a global synthesis *Cambride Univer. Press* .
- Moreira-Turcq P, Seyler P, Guyot J L Etcheber H 2003 Exportation of organic carbon from the Amazon River and its main tributaries *Hydrol. Process.* **17** 1329-1344.

- 1  
2  
3 Mouyen M, Longuevergne L, Steer P, Crave C, Lemoine J, Save H, Robin C 2018  
4 Assessing modern river sediment discharge to the ocean using satellite gravimetry  
5 Nat. Commun. **9** 3384.  
6  
7 Nobre C A, Sampaio G, Borma L S, Castilla-Rubio J C, Silva J S, Cardoso M 2016  
8 Land-use and climate change risks in the Amazon and the need of a novel  
9 sustainable development paradigm *PNAS* **39** 10759-10768.  
10  
11 Pepin E, Guyot J L, Armijos E, Bazán H, Fraizy P, Moquet J S, Vauchel P 2013  
12 Climatic control on eastern Andean denudation rates Central Cordillera from  
13 Ecuador to Bolivia *J. South Am. Earth Sci.* **44** 85-93.  
14  
15 Picouet C, Hingray B, Olivry J C 2001 Empirical and conceptual modelling of the  
16 suspended sediment dynamics in a large tropical African river: the Upper Niger  
17 river basin *J. Hydrol.* **2501** 19-39.  
18  
19 Pontes P R, Collischonn W, Fan F M, Paiva R C, Buarque D C 2015 Modelagem  
20 hidrológica e hidráulica de grande escala com propagação inercial de vazões *Rev.*  
21 *Brasil. Recu. Hidrol.* **204** 888-904.  
22  
23 Richey J E, Meade R H, Salati E, Devol A H, Nordin Jr C F, Santos U D 1986 Water  
24 discharge and suspended sediment concentrations in the Amazon River: 1982–  
25 1984. *Water. Resour. Res.* **22** 5 756-764.  
26  
27 Salati E and Vose P B 1984 Amazon basin: A system in equilibrium *Scienc.* **225** 4658.  
28  
29 Santini W, Martinez J M, Guyot J L, Espinoza R, Vauchel P, Lavado W 2014  
30 Estimation of erosion and sedimentation yield in the Ucayali river basin a  
31 Peruvian tributary of the Amazon River using ground and satellite methods *EGU*  
32 **16**.  
33  
34 Vauchel P, Santini W, Guyot J L, Moquet J S, Martinez J M, Espinoza J C, Baby P,  
35 Fuertes O, Noriega L Puita O, Sondag F, Fraizy P, Armijos E, Cochonneau G,  
36 Timouk F, Oliveira E, Filizola N, Molina J, Ronchail J 2017 A reassessment of  
37 the suspended sediment load in the Madeira River basin from the Andes of Peru  
38 and Bolivia to the Amazon River in Brazil based on 10 years of data from the  
39 HYBAM monitoring programme *J. Hydrol.* **553** 35-48.  
40  
41 Walling D E and Webb B W 1982 Sediment availability and the prediction of storm-  
42 period sediment yields *Recent develop. explanat. and predict. erosion and*  
43 *sediment* **137** 327-337.  
44  
45  
46  
47  
48  
49  
50  
51  
52  
53  
54  
55  
56  
57  
58  
59  
60